

Characterization and Functionality of Proliferative Human Sertoli Cells

Kitty Chui,^{*1} Alpa Trivedi,^{*†1} C. Yan Cheng,[‡] Diana B. Cherbavaz,^{*}
Paul F. Dazin,^{*} Ai Lam Thu Huynh,^{*} James B. Mitchell,[§]
Gabriel A. Rabinovich,[¶] Linda J. Noble-Haeusslein,[†] and Constance M. John^{*}

^{*}MandalMed, Inc., San Francisco, CA, USA

[†]Department of Neurosurgery, University of California, San Francisco, CA, USA

[‡]Population Council, New York, NY, USA

[§]Lonza Walkersville, Walkersville, MD, USA

[¶]Laboratory of Immunopathology, Institute of Biology and Experimental Medicine, CONICET, Buenos Aires, Argentina

It has long been thought that mammalian Sertoli cells are terminally differentiated and nondividing postpuberty. For most previous *in vitro* studies immature rodent testes have been the source of Sertoli cells and these have shown little proliferative ability when cultured. We have isolated and characterized Sertoli cells from human cadaveric testes from seven donors ranging from 12 to 36 years of age. The cells proliferated readily *in vitro* under the optimized conditions used with a doubling time of approximately 4 days. Nuclear 5-ethynyl-2'-deoxyuridine (EdU) incorporation confirmed that dividing cells represented the majority of the population. Classical Sertoli cell ultrastructural features, lipid droplet accumulation, and immunorexpression of GATA-4, Sox9, and the FSH receptor (FSHR) were observed by electron and fluorescence microscopy, respectively. Flow cytometry revealed the expression of GATA-4 and Sox9 by more than 99% of the cells, and abundant expression of a number of markers indicative of multipotent mesenchymal cells. Low detection of endogenous alkaline phosphatase activity after passaging showed that few peritubular myoid cells were present. GATA-4 and SOX9 expression were confirmed by reverse transcription polymerase chain reaction (RT-PCR), along with expression of stem cell factor (SCF), glial cell line-derived neurotrophic factor (GDNF), and bone morphogenic protein 4 (BMP4). Tight junctions were formed by Sertoli cells plated on transwell inserts coated with fibronectin as revealed by increased transepithelial electrical resistance (TER) and polarized secretion of the immunoregulatory protein, galectin-1. These primary Sertoli cell populations could be expanded dramatically *in vitro* and could be cryopreserved. The results show that functional human Sertoli cells can be propagated *in vitro* from testicular cells isolated from adult testis. The proliferative human Sertoli cells should have important applications in studying infertility, reproductive toxicology, testicular cancer, and spermatogenesis, and due to their unique biological properties potentially could be useful in cell therapy.

Key words: Sertoli cells; Blood–testis barrier (BTB); Sox9; Galectin-1

INTRODUCTION

Somatic Sertoli cells are the main structural component of the seminiferous tubule, create the blood–testis barrier (BTB), and perform multiple functions that are required for the remarkable cellular transformation of spermatogonial stem cells into haploid cells and then into spermatozoa (22). Although often termed “mother” or “nurse” cells because of their role in nurturing the developing germ cells, Sertoli cells also are important as phagocytes of the residual cytoplasm of more than

half of the differentiating germ cells that undergo apoptosis.

The BTB that is formed by tight junctions between the Sertoli cells is thought to limit the access of nutrients, hormones, and other biological substances to the adluminal compartment of the seminiferous tubule, and to physically shield the postmeiotic germ cells from the immune system (64,87). Sertoli cell expression of various mediators also is thought to create a localized immunosuppressive effect within the testis (18,59). The ability of Sertoli cells to modulate immune responses has been

Received July 22, 2010; final acceptance September 26, 2010. Online prepub date: November 5, 2010.

¹These authors provided equal contribution to this work.

Address correspondence to Constance M. John, Ph.D., MandalMed, Inc., 665 3rd Street, Suite 250, San Francisco, CA 94107, USA. Tel: (415) 495-5570; Fax: (415) 495-5575; E-mail: constancejohn@mandalmed.com

studied by cotransplanting them with other cells at ectopic sites, where Sertoli cells were found to protect and extend survival of such grafts (16,37,56,59,68).

During fetal and early postnatal development in mice, the transcription factor GATA-4, a zinc finger protein implicated in regulation of gene expression and cellular differentiation, is expressed in the Sertoli and Leydig cells but not germ cells (34,38,79). Another protein expressed by immature and mature Sertoli cells is Sox9 (30,35,36). Sox9 (34) and FSHr (4) are both exclusively expressed by Sertoli cells in the testis. Sox9 is a Sry-box-containing gene encoding a transcriptional activator that has been found to suffice for testis formation in mice (33), is essential for Sertoli cell differentiation (20,30,45,46), and has been used to identify Sertoli cells in transplantation studies (25). Immunoreactivity has shown that human Sertoli cells produce GDNF, which is thought to aid in the self-renewal of spermatogonial stem cells (11,26), and immunohistochemical analyses also have shown that galectin-1 is expressed by rat (13) and human Sertoli cells (83).

It has long been thought to be a fact that mammalian Sertoli cells do not divide postpuberty (49,62). For many *in vitro* studies, testes from immature 20-day-old rodent pups have been the source of Sertoli cells (77) and these have shown little proliferative ability. The rodent Sertoli cells have been thought to cease dividing by postnatal day 15–17 when the BTB is being established (8). We unexpectedly discovered (75) that human Sertoli cells from adult humans regain proliferative ability *in vitro* using standard cell culture conditions and medium containing fetal bovine serum (FBS) but no other additives such as hormones or gonadotropins. Our findings are supported by those of Ahmed et al. (1), who reported that Sertoli cells isolated from the adult mouse and human testis resume proliferation in culture in the absence of hormonal supplementation.

Because there is interest in using Sertoli cells to minimize transplant rejection due to their inherent immunological suppressive properties (17,61), establishing conditions to produce proliferative human Sertoli cells *in vitro* could facilitate research on their use for therapeutic applications, such as in cell or organ transplantation. In this study, we specifically aimed to reproducibly isolate, and expand primary adult human Sertoli cells from cadaveric testes, and then to characterize the cells and to determine their functionality *in vitro*.

MATERIALS AND METHODS

Isolation and Culture of Human Sertoli Cells

Seven deceased individuals (12–36 years of age) were donors of testicular tissue that was obtained from the National Disease Research Interchange (NDRI, Philadelphia, PA, USA) within 36 h of death. The isolation

protocol was a modification of a previously described method (39), and was approved by the Committee on Human Research, University of California (San Francisco, CA, USA). All reagents and materials were handled aseptically. The testis was washed with ice-cold calcium/magnesium free Hanks balanced salt solution (HBSS) containing 100 U/ml penicillin and 100 µg/ml streptomycin, and then all of the skin and the tunica albuginea were removed. The tissue was rinsed again with HBSS, minced, transferred to a 1-L Erlenmeyer flask, and washed three times with HBSS. After the final wash, the tissue was covered with HBSS, transferred to a 37°C water bath, and shaken at 275–325 rpm for 15 min. Again, the tissue was allowed to settle, and the supernatant was discarded, and 100 ml of HBSS containing 0.25% trypsin (Sigma, St. Louis, MO, USA), and 0.1% collagenase type IV (Sigma) was added. The flask was shaken at 275–325 rpm in a water bath at 37°C for 20 min, the solution was strained through a coarse wire mesh (1 mm²) and the flow-through stored on ice. If undigested tissue remained, the digestion was repeated. Finally, 0.034% of soybean trypsin inhibitor (Sigma) was added, the homogenate was passed through a syringe with an 18-gauge needle, and then centrifuged at 800 × *g* for 5 min. The cell pellet was suspended in DMEM/F-12 Hams medium [1:1; Cell Culture Facility, University of California, San Francisco (UCSF)], containing penicillin and streptomycin, with 5% FBS, and plated in a T-225 flask. The cells were propagated in the same medium and incubated at 37°C in a 5% CO₂ incubator. Cells were dissociated using Cell Dissociation Buffer (Invitrogen, Carlsbad, CA, USA) and trypsin (0.05%) with EDTA.

Ultrastructural Analysis by Transmission Electron Microscopy

Cells at 70–80% confluence were rinsed with 0.1 M sodium cacodylate buffer, pH 7.4, and fixed with buffered 2% glutaraldehyde. Samples, collected by scraping the dishes, were pelleted at 800 × *g* for 2 min, and post-fixed with 1% osmium tetroxide. Pelleted cells were dehydrated in graded ethanol solutions, infiltrated, and embedded in Epon-Araldite-812 (Electron Microscopy Science, Fort Washington, PA, USA). Sections were cut at 70-nm thickness using a diamond knife, stained with uranyl acetate and lead citrate, and imaged at 4,000–25,000 magnification on a Zeiss EM 10C Electron 5 microscope.

Immunocytochemical Analysis

Sertoli cells were grown on glass chamber slides (LabTek II, Nunc; Thermo Fisher, Rochester, NY, USA) and fixed with methanol at –80°C for 1 h or 4% paraformaldehyde (PFA) at room temperature (RT) for 30

min. After washing with phosphate-buffered saline (PBS), the cells were blocked and permeabilized by incubation in 2–5% normal serum in PBS with 0.1–0.2% Triton X-100 at RT for 1 h. Cells were incubated with primary antibodies (Table 1) that were diluted in blocking buffer at 4°C overnight. Dye-conjugated secondary antibodies were diluted in blocking buffer, and incubated at RT for 1 h. The controls were: cells without antibody, secondary antibody alone, and nonspecific IgG (control for primary antibody) with secondary antibody. Cell nuclei were stained with bisbenzamide (Invitrogen, 2 µg/ml) for 2 min, washed with PBS, and mounted using Aqua-Mount (Biomedex, Foster City, CA, USA). Images from fluorescence microscopy were captured with NIS-Elements v.2 software with cooled CCD camera, with image processing and pseudocolor enhancement of contrast (Photoshop, Adobe, San Jose, CA, USA or ImageJ).

Cell Expansion and Storage

For expansion, viable cells were counted by trypan blue exclusion using a hemacytometer, seeded (1×10^5 cells) in a T-225 tissue culture flask, and propagated in DMEM/F-12 Hams medium (1:1; Cell Culture Facility, UCSF) with 5% FBS in a 5% CO₂ incubator at 37°C. When 80–90% confluent, cells were harvested with Cell Dissociation Buffer (Invitrogen) and trypsin (0.05%) with EDTA, and stored in liquid nitrogen in dimethyl sulfoxide-containing Cell Preservation Media (Cell Culture Facility, UCSF). After cryopreservation, cells were thawed and seeded at 4.5×10^2 cells/cm². The number of viable cells and cell seeding efficiency were quantified. Viability was based on trypan blue exclusion and seed-

ing efficiency was determined by quantifying nonviable floating cells after 72 h in cell culture media. The division rate was calculated by plating (4.5×10^2 cells/cm²) and quantifying cells over nine or more divisions to determine an average rate. In addition, the division rate and contact inhibition were examined by quantifying the increase in metabolically active cells plated in 96-well plates over a 48-h period.

Detection of Proliferation by Incorporation of 5-Ethynyl-2'-Deoxyuridine

To evaluate cell proliferation, 3.6×10^4 cells were added to each well of a four-well chamber slide, and allowed to attach overnight. Cells were incubated with 2 µM 5-ethynyl-2'-deoxyuridine (EdU) in 0.5 ml medium at 37°C in a 5% CO₂ incubator for 3 days. The cells were washed twice with HBSS, allowed to recover overnight, and then fixed in methanol at –80°C overnight. The cells were blocked by washing twice with 5% normal goat serum in PBS, permeabilized in 0.5% Tween-20 in PBS at RT for 20 min, and then washed twice with blocking buffer. For detection, 150 µl of the Alexa-Fluor 594-conjugated azide cocktail (Invitrogen) was added (per the manufacturer's instructions) per well and the slide rocked in the dark at RT for 30 min. Cells were washed twice before the slides were mounted.

Lipid Droplet Staining of Sertoli Cells

Lipid droplets were stained by adding 30 µl of AdipoRed (Lonza, Walkersville, MD, USA) per ml of PBS. The AdipoRed solution was added to cells growing on coverslips or chamber slides after washing with PBS and then the cells were incubated at RT for at least 10 min.

Table 1. Antibodies Used in the Study

Target	Source	Catalog No.	Host	Type*	Application	Dilution
GATA-4	Santa Cruz Biotechnology	Sc-9053	rabbit	pAb	IF, FACS	1:50 (IF)
Sox9	Santa Cruz Biotechnology	Sc-17341	goat	pAb	IF, FACS	1:50 (IF)
FSHr	ABD Serotec	4561-8019	sheep	pAb	IF	1:3000 (IF)
CD13	Invitrogen	MHCD1301	mouse	mAb	FACS	1:20
CD14	Invitrogen	MHCD1401	mouse	mAb	FACS	1:20
CD29	Invitrogen	CD2901	mouse	mAb	FACS	1:20
CD31	BD Biosciences	555446	mouse	mAb	FACS	1:5
CD34	BD Biosciences	348057	mouse	mAb	FACS	1:5
CD44	Invitrogen	MHCD4404	mouse	mAb	FACS	1:20
CD45	Invitrogen	MHCD4501	mouse	mAb	FACS	1:20
CD73	BD Biosciences	550257	mouse	mAb	FACS	1:5
CD90	BD Biosciences	555595	mouse	mAb	FACS	1:50
CD105	Invitrogen	MHCD10504	mouse	mAb	FACS	1:20
CD166	BD Biosciences	559263	mouse	mAb	FACS	1:5
Gal-1	Rabinovich	N/A	rabbit	pAb	IB, IHC	1:3000

*pAb, polyclonal; mAb, monoclonal.

After rinsing again with PBS, the slides were mounted, and Cy3 fluorescence was visualized on the Nikon TE2000E epifluorescence microscope (excitation 510–550 nm and emission 590 nm).

Analysis of Endogenous Alkaline Phosphatase Activity From Myoid Cells

Testicular cells (passage 4) growing on glass chamber slides were rinsed with PBS, fixed in 4% PFA in PBS for 1–2 min, and rinsed with buffered saline solution. The Vector Red substrate (Vector Labs, Burlingame, CA, USA) was prepared according to the manufacturer's instructions. The substrate solution was added to the cells and incubated at RT in the dark for 20–30 min. After rinsing with buffered saline solution, the slides were mounted, and the cells analyzed by light and fluorescence microscopy.

Proliferation and Contact Inhibition

To further quantify cell proliferation and assess contact inhibition, 0.5×10^3 , 1.0×10^3 , 2.0×10^3 , or 4.0×10^3 (1,500–12,000/cm²) MM-HSE-2305 cells (passage 5) were plated in 96-well tissue culture plates and incubated at 37°C in a 5% CO₂ incubator. The relative number of cells per well was determined from absorbance due to the active metabolism of the cell proliferation reagent WST-1 (Roche, Indianapolis, IN, USA) according to the directions of the manufacturer. At 24 h postplating the above-mentioned numbers of cells, 10 µl of WST-1 was added to control wells and the absorbance was measured 2 h after it was added. The WST-1 absorbance was measured at 450 nm on a Thermomax microplate reader (Molecular Devices, Sunnyvale, CA, USA). Total cell numbers were quantified in quadruplicate wells and defined as 100%. Background from the slight spontaneous absorption of medium alone with WST-1 was subtracted from the reading for each well. At 72 h postplating, another set of quadruplicate wells was analyzed with WST-1 as above. Proliferation over a 48 h-period was assessed by comparing the WST-1 absorbance of wells analyzed at 24 h to that of wells analyzed at 72 h postplating. The experiment was repeated three times.

Gene Expression Profiles of Sertoli Cells by RT-PCR

RT-PCR primer sets were designed to investigate the mRNA expression profiles of the cells (Table 2) as described. Total RNA was extracted from MM-HSE-3608 and MM-HSE-1208 cells using an RNeasy minikit from Qiagen (Valencia, CA, USA). To assess the RNA quality, the ratios of r18S to r28S ribosomal RNA were analyzed on a RNA Nano 6000 chip (Bioanalyzer 2100, Agilent, Santa Clara, CA, USA), and found to be 1.98 and 2.19, respectively. Genomic DNA was eliminated

using RT2 First Strand kit (SA Biosciences, Frederick, MD, USA). For reverse transcription of the first-strand cDNA, the primers were added to 5 µg of total RNA in a total 20-µl reaction volume. The cDNA solution (1 µl) was added to 10 µl of the 2× Fast Cycling PCR mix (Qiagen) along with 4 µl of the 5× Q solution, and 10 µM of the corresponding primer set for a final 20-µl volume. PCR conditions were 5 min denaturation at 95°C, followed by 35 cycles at 96°C for 5 s, 55°C or 60°C annealing for 5 s, and extensions at 54–68°C for 9 s, with a final extension of 68°C for 5 min. The PCR products were resolved with either a 1.2% or 2% Sybr Safe stained E-gel (Invitrogen), and were visualized by a UV transilluminator equipped with Canon S5 IS digital camera mounted onto a Spectroline portable dark room system (Spectronics, Westbury, NY, USA).

Fluorescence-Assisted Cell Sorting (FACS)

For FACS, the antibodies against Sox9 and GATA-4 (gelatin-free; Santa Cruz Biotechnology, Santa Cruz, CA, USA) were conjugated to allophycocyanin using a kit (Lightning-Link Allophycocyanin-XL kit, Innova Biosciences, Cambridge, UK) according to the instructions of the vendor. Glycerol (60 µl) was added to each vial to extend the shelf life of the antibodies and aliquots were placed at –80°C for long-term storage. Cells of passage 3–4 were harvested for FACS, centrifuged (800 × g for 10 min) to form a pellet with approximately 1×10^7 cells, and the supernatant was removed. The cells were washed in PBS and a single cell suspension was formed in 5% cell dissociation buffer, 2% FBS, and 0.05% Triton X-100 by gentle pipetting. Cold (–80°C) methanol was added (1 ml for 1×10^6 cells) and the cells were placed at –80°C from 1 h to overnight. After centrifugation (200 × g for 5 min), the supernatant was removed, and the cells were incubated with primary antibody or controls (nonspecific species-matched allophycocyanin-labeled polyclonal antibody; 0.5 µl APC-antibody conjugate solution per 0.5–1.0 million cells, or buffer alone) in 0.5 ml of blocking buffer (PBS with 0.1% Triton X-100 and 5% cell dissociation buffer and 5% species-specific serum, for example, goat serum with goat anti-Sox9 antibody) in the dark at RT for 1 h. The cells were washed twice with 2 ml of wash buffer per tube, pelleted by centrifugation (200 × g for 5 min), the supernatant removed, and, lastly, the cells were suspended in 0.5 ml wash buffer for analysis.

For staining cell surface antigens, cells of passage 3–4 were pelleted by centrifugation, and suspended in 1.2 ml of blocking buffer [PBS with 5% normal goat serum, 0.1% bovine serum albumin, 0.01% sodium azide (Sigma)] and incubated on ice for 10 min. Approximately 1×10^6 cells were distributed in 100-µl aliquots into 11 5-ml tubes, and stained with monoclonal anti-

Table 2. Sequence of Primers for RT-PCR

Gene	Forward Primer	Reverse Primer	Accession	Start	End	BP	T	T _m
Sox9	GAGCGAGGAGGACAAGTTC	CATGAAGGCGTTCATGGGC	37704387	561	711	151	58	55
GATA-4	CTAGACCGTGGGTTTTGCAT	GCAGTCGTCTTCTTCCAGG	172072611	2188	3030	843	60	60
GDNF	GGGCACCTGGAGTTAATGTC	TCTGGAATCTCTGGGTTGG	40549401	124	512	389	60	60
SCF	GCTCCAGAACAGCTAAACGG	TCTTTGACGCACTCCACAAG	337933	117	533	417	60	60
Oct4	CGTGAAGCTGGAGAAGGAGAAGCTG	CAAGGGCCGCAGCTCACACATGTT	12382251	363	607	245	68	60
Nanog	GCTTGCCCTTGCTTTGAAGCA	TTCTTGACTGGGACCTTGTC	13376297	245	500	256	58	55
BMP4	AGCCATGCTAGTTTGATAACC	CGATCGGCTAATCCTGACAT	576934	147	854	708	54	55
GAPDH	ACCCAGAAGACTGTGGATGG	TTCAGCTCAGGGATGACCTT		653	777	125	60	60

BP, number of base pairs; T, extension temperature; T_m, annealing temperature.

bodies for CD13, CD29, CD34, CD44, CD73, CD90, CD105, and CD166 or isotype control mAbs while incubating on ice in the dark for 30 min. The isotype control monoclonal antibodies were specific to each antibody pair (mouse IgG_{2b} PE; BD Biosciences, San Jose, CA, USA) for CD44 and IgG₁ FITC, IgG₁ PE (Invitrogen) for the remaining monoclonal antibodies. In addition, monoclonal antibodies to CD13 and CD73 were run independently as FL-1 and FL-2 compensation controls, respectively. All antibodies were run at approximately 10 µg/ml concentration including isotype controls. The cells were washed two times in 2 ml FACS wash buffer (200 × g for 5 min) then fixed in 200 µl of 1% PFA. Data acquisition was performed on 10,000 events per tube based on a total (ungated) count of forward and side light scatter at approximately 200–300 events/s on a BD FACSort flow cytometer (BD Biosciences) and analyzed using CELLQuest Pro software (BD Biosciences).

Formation of Polarized Sertoli Cell Monolayers

Transwell inserts (0.4 µm pore size, 0.33 cm² surface area, PET, Corning, Lowell, MA, USA) were coated with 100 µl of 6.6 µg/ml human fibronectin (BD Biosciences) diluted in PBS at RT overnight. Sertoli cells (passage 4–5) were harvested and seeded at a cell density of 5 × 10⁵ cells in 300 µl medium in the apical chamber with 900 µl medium in the basolateral chamber of each 24-well transwell insert. After 7 days, TER was measured in three positions on each insert using a MilliCell Electrical Resistance System (ERS) epithelial volt ohmmeter equipped with an Ag/Ag electrode (STX2, World Precision Instruments, Sarasota, FL, USA). Raw data were normalized by subtracting the TER of control matrix-coated wells without cells. Experiments also were performed with Sertoli cells on inserts coated with Matrigel (BD Biosciences), and on transwell inserts pre-coated with collagen I, laminin, or fibronectin (BioCoat; BD Biosciences).

Immunohistochemistry of Galectin-1 in Adult Testis

The expression of galectin-1 in normal human testis was determined by fluorescence immunocytochemistry on cryosections of human testis tissue stained using the ABC Elite system (Vector Labs). Normal testicular tissue was obtained from the National Disease Research Interchange (Philadelphia, PA, USA) and fixed by incubation in 3% PFA overnight. Fixed tissue was processed at the Histology Core of the J. David Gladstone Institutes (San Francisco, CA, USA) where cryosections were prepared of 15-µm thickness and collected onto Superfrost slides. The cryosections were fixed by incubation in cold methanol at –80°C for 5 min. The samples were rehydrated with PBS, and blocked with 10% horse serum in PBS with 0.1% Triton-X-100 (PBST) at RT for 30 min, and then with biotin-avidin blocking buffer (Vector Labs) for 30 min. Primary antibody was diluted 1:200 in protein-free blocking buffer and sections were incubated at 4°C overnight. After washing with PBST, sections were incubated with biotinylated secondary antibody (biotinylated universal anti-IgG of rabbit/mouse/goat) at room temperature for 30 min. After washing again three times with PBST, the sections were incubated with DyLight Streptavidin 488 at room temperature for 20 min. Finally, the samples and controls were washed three times with PBST, mounted, and visualized.

Immunoblot for Galectin-1

Sertoli cells (MM-HSE-3608) were seeded onto fibronectin-coated 24-well transwell chambers to form polarized monolayers as described above. Media from the apical (top) and basal (bottom) chambers were collected at 3 and 7 days and analyzed by SDS-PAGE and immunoblot. Equal volumes of conditioned media from the chambers were resolved on 4–12% NuPAGE® Novex® Bis-Tris gel (Invitrogen) with 2-(N-morpholino) ethanesulfonic acid (MES) SDS buffer at 200 V for 35 min. Proteins were electrotransferred onto 0.2 µm nitro-

cellulose membrane (30 V for 1 h). The transfer efficiency was confirmed by Ponceau S staining. After incubation with protein-free blocking buffer (Thermo/Pierce) at 4°C overnight, blots were incubated with diluted galectin-1 polyclonal antibody (1:3,000–1:5,000) at RT for 1 h, washed with TBS-Tween five times, and incubated with diluted horseradish peroxidase (HRP) 1:5,000–1:10,000 at RT for 1 h. After washing five times with TBS-Tween, the blot was rinsed in water, developed with TMB and membrane enhancer (KPL). Images were captured with a digital camera and digitally enhanced (Adobe PhotoShop or ImageJ).

Effect of Conditioned Medium From Human Sertoli Cells on Lymphocyte Proliferation

Conditioned media were collected from MM-HSE-2305 and human foreskin fibroblast (control) cell line Hs27 (CRL-1634; ATCC, Manassas, VA, USA) cultures at 70–80% confluency at 48 h postplating. The experiments were performed in a 96-well plate. Each assay well had a total volume of 120 μ l, with 1×10^4 human lymphocytes (ATCC; Jurkat E6-1, TIB-152) maintained in RPMI-1640 media with 15% FBS, $1 \times$ penicillin-streptomycin) with varying amounts of either Sertoli or Hs27 fibroblast conditioned media or unconditioned medium (serving as controls). The 96-well plate was incubated at 37°C in a 5% CO₂ incubator for 72 h. The relative proliferation of the lymphocytes in each well was then determined by active metabolism of WST-1. After 2–4 h of incubation with 12 μ l of WST-1 according to the directions of the manufacturer, the absorbance was measured at 450 nm. The absorption of the medium alone with WST-1 defined as background was subtracted from the reading for each well.

Statistical Analyses

Multiple group comparisons were analyzed by one- and two-way ANOVA followed by Bonferroni's post hoc analysis (GraphPad Prism, Version 4.03). Within-group comparisons were done using two-tailed *t*-tests. Data are expressed as mean \pm SD. Significance was defined at $p < 0.05$.

RESULTS

Sertoli Cell Isolation and Ultrastructural Characterization

At 2–20 days postisolation from the testis tissue, a few thin cells were observed adherent to the bottom of culture flasks. Initially, less than approximately 20 distinct colonies of cells were apparent with each colony comprising only a few cells. The numbers of cells within the colonies expanded beyond what was seen within the first several days after plating, consistent with cell proliferation. Cells typically assumed polygonal phenotypes with irregularly shaped nuclei and several filamentous

processes of variable length extending outward from the cell bodies (Fig. 1A, B). Their morphology was similar to that of the Sertoli cells that we previously isolated from neonatal rats (77).

The cells continued to divide until reaching confluence in the flask, typically after 3–4 weeks, when they were passaged (4.5×10^2 cells/cm²). In general the morphology of the cells was unchanging with passage as can be seen by comparing MM-HSE-3608 cells from passage 2 (Fig. 1A) and passage 4 (Fig. 1B); however, the average cell size appeared to increase slightly. It was confirmed that after cryopreservation, cells of low passage number (passage 1–5) could be refrozen, thawed, and replated.

Ultrastructural analyses also revealed morphology consistent with that of Sertoli cells (Fig. 1C–F). The large irregularly shaped nuclei of most cells had prominent nucleoli. Other features typical of Sertoli cells could be observed including lipid droplets, abundant smooth and rough endoplasmic reticulum, and perinucleolar spheres.

Cells Exhibit Contact Inhibition and Proliferate in Culture

Three separate analyses of viability, seeding efficiency, and division rate (Table 3) were performed after cryopreservation of vials of cells isolated from tissues from two donors, termed MM-HSE-3608 (passage 2) and MM-HSE-2305 (passage 3) as described in Materials and Methods. Cryopreserved cells retained about 90% viability, 83% seeding efficiency, and had an average division rate of 4 days. The results presented (Table 3) are the mean \pm SD of independent assays of three vials of cryopreserved MM-HSE-2305 and MM-HSE-3608 cells with duplicate or triplicate analyses. The cells retained the ability to proliferate after prolonged cryostorage (>30 months) and multiple freeze–thaw cycles.

A doubling rate of approximately 4 days was also determined by quantifying and comparing the number of metabolically active cells in 96-well plates at 24 and 72 h postplating (Fig. 2). Contact inhibition was observed as when plated at high densities (4×10^3 cells/well), the cells did not proliferate, thereby demonstrating their nontransformed nature. The cells maintained contact inhibition after multiple passages and prolonged culture.

The incorporation of EdU (Invitrogen) into the nucleus of dividing cells over a 3-day period was used to assess cell proliferation directly. MM-HSE-3608 cells (passage 6) were incubated with EdU that was incorporated into DNA during active synthesis. Fluorescent detection was enabled by reaction of the EdU-conjugated alkyne with azide linked to Alexa-Fluor 594 (Click-iT® EdU, Invitrogen). Phase contrast images showed the cell boundaries were overlaid with fluorescence images (Fig.

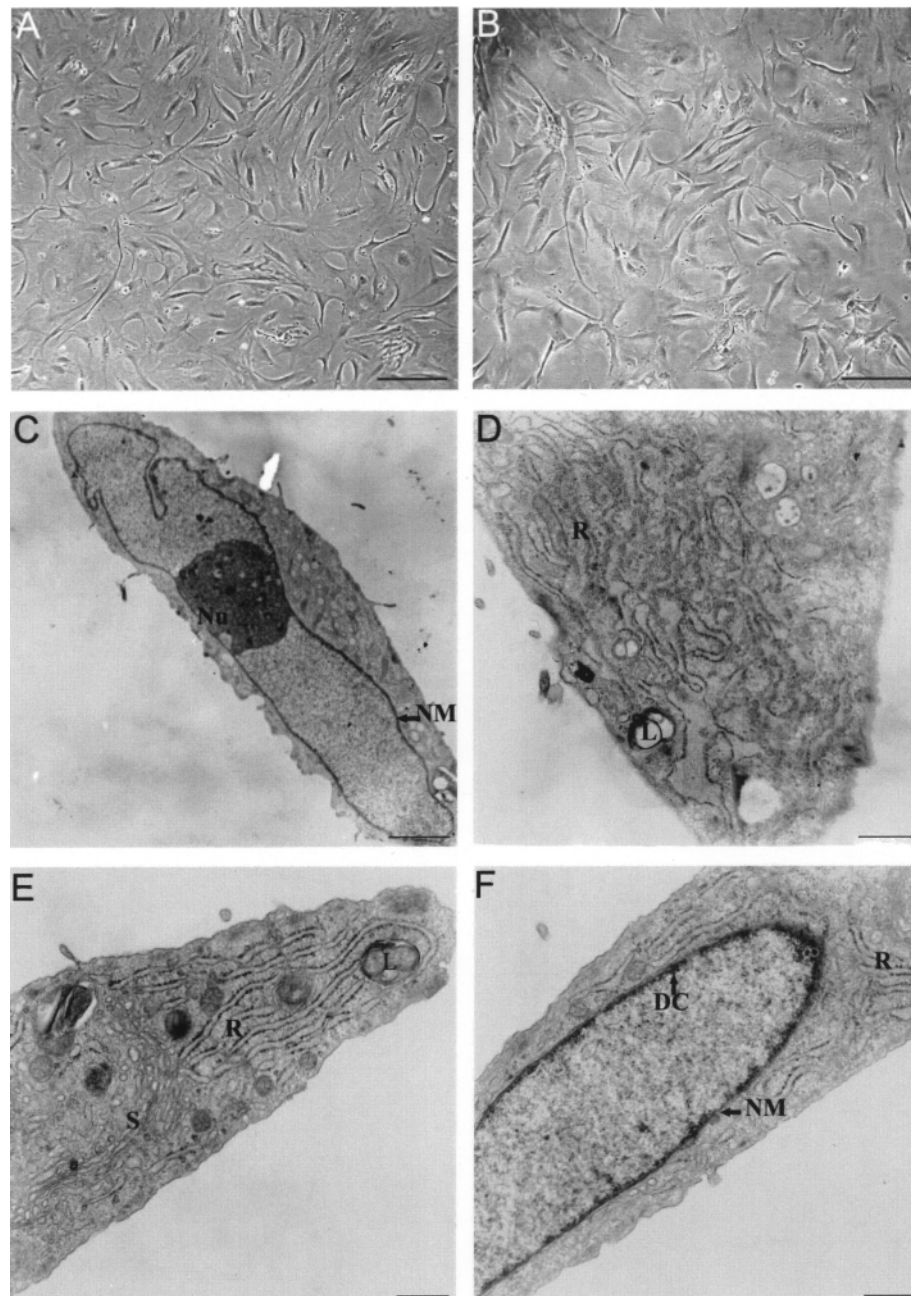


Figure 1. Morphology consistent with Sertoli cells shown by cultured cells. Phase contrast microscopy of MM-HSE-3608 cells of passage 2 (A) and passage 4 (B) reveals features characteristic of Sertoli cells including branching cytoplasmic processes and irregularly shaped nuclei. Electron microscopy of MM-HSE-2305 cells of passage 2 (C–F) clearly shows the irregularity of the shape of the nucleus (NM; nuclear membrane) in addition to the prominent nucleolus (Nu). Lipid droplets (L) and abundant rough (R) and smooth (S) endoplasmic reticulum are evident within the cytoplasm (D, E). Dense chromatin (DC) is apparent along the nuclear envelope (F). Scale bars: 200 μm (A, B), 2.3 μm (C), 750 nm (D), 500 nm (E, F).

Table 3. Cryopreserved Vial Analysis

Assay	3608 P2	2305 P3
Viability (%)	88.0 ± 5.41	91.1 ± 3.87
Seeding (%)	83.3 ± 10.2	83.0 ± 9.90
Division (day)	4.51 ± 0.35	3.32 ± 0.35

Duplicates in three separate experiments with \pm SD. Trypan blue exclusion for viability; divisions of >9 twice plating 450 cells/cm². P, passage number.

3A), revealing that the majority of nuclei were stained red, indicating incorporation of EdU.

Immunological and Histological Analyses

The presence of lipid droplets is a salient feature of Sertoli cells from humans (51,58) and other mammalian species (31) that can be easily detected by the Oil red O-based method (81) (Lonza). The presence of lipid is shown by lighter spots of various sizes in the cytoplasm of cells in the grayscale image in Figure 3B. The appearance of the droplets is similar to that observed in murine Sertoli cells in coculture with germ cells (81).

Isolated cells were found to express GATA-4 (Fig. 3C) and FSHr (Fig. 3D). High and low concentrations of primary antibodies demonstrated dose-dependent specificity and antigen-specific staining patterns. GATA-4 was

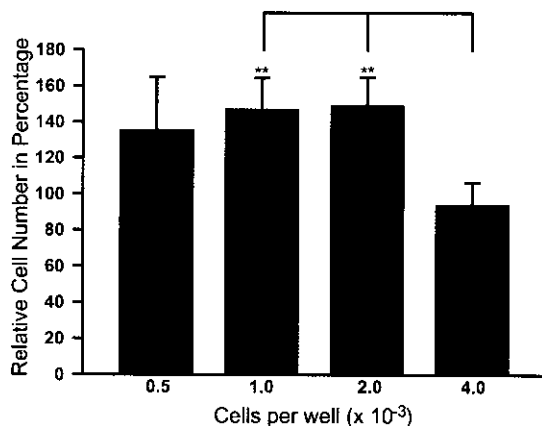


Figure 2. Percentage increase in number of Sertoli cells (MM-HSE-2305; P5) at 72 h postplating compared to the number of cells in control wells at 24 h postplating. There was a significant difference in the proliferation of the cells (indicated by bar, $p < 0.0001$) plated at 1.0 or 2.0 $\times 10^3$ cells per well and those that were plated at 4.0 $\times 10^3$ cells per well based upon one-way ANOVA. The number of cells initially plated (assessed at 24 h) at 1.0 and 2.0 $\times 10^3$ cells per well increased significantly by almost 50% over 48 h (** $p = 0.004$). The results are the mean of two independent experiments with quadruplicates, and are representative of three independent experiments.

localized to the nucleus as expected for a transcription factors whereas FSHr staining also as expected was cytoplasmically localized.

Alkaline phosphatase is expressed by the peritubular myoid cells but not Sertoli cells (2). However, relatively few myoid cells were stained for endogenous alkaline phosphatase activity as illustrated in Figure 3E, and the number of stained cells diminished with increasing passage. These data alleviated a concern that myoid cells could overtake the cultures in the FBS-containing growth medium.

MM-HSE-2305 Cells Express Several Genes Typical of Sertoli Cells

RT-PCR analysis of MM-HSE-2305 cells revealed that they expressed several typical genes previously shown to be expressed by Sertoli cells. Consistent with previously published results, the human Sertoli cells expressed stem cell factor (SCF) (57,67), glial cell line-derived neurotrophic factor (GDNF) (11,26), and bone morphogenic protein 4 (BMP4) (27). GAPDH, a housekeeping gene, was used as a control (5). The PCR product sizes (Fig. 4) matched computer predictions from NCBI sequence data. Lane 1 presents analysis of MM-HSE-3608 cells, and lane 2 of MM-HSE-1208 cells. No PCR products were detected in the no-RNA control sample (data not shown).

Flow Cytometric Analysis Reveals Expression of Sertoli Cell Markers

The results from flow cytometry of human Sertoli cells from two different donors, MM-HSE-3608 (passage 3) and MM-HSE-2305 (passage 4) cells were very similar (Fig. 5A, B). The cells positively staining for GATA-4 and Sox9 in 3608 and 2305 were more than 99% of the population confirming the Sertoli cell identity of most cells. Similarly, flow cytometric analysis of MM-HSE-1208 (passage 4) and MM-HSE-1509 cells (passage 4) isolated from two other donors revealed that 98.7% and 97.5% expressed Sox9, respectively, and 95.5% and 96.9% of the cells expressed GATA-4, respectively (data not shown).

The MM-HSE-3608 and MM-HSE-2305 cells were negative for CD34 (4% and 6%, respectively), which is expressed by hematopoietic and endothelial progenitor cells (71), and were of mixed expression for CD13 (82% and 95%, respectively), CD90 (98 and 70%, respectively), and CD166 (82% and 99%, respectively). Interestingly, the two populations, MM-HSE-3608 and MM-HSE-2305, were almost uniformly expressive of a number of markers: CD29 (99 and 100%, respectively), CD44 (98 and 99%, respectively) CD105 (98 and 99%, respectively), and CD73 (98 and 99%, respectively).

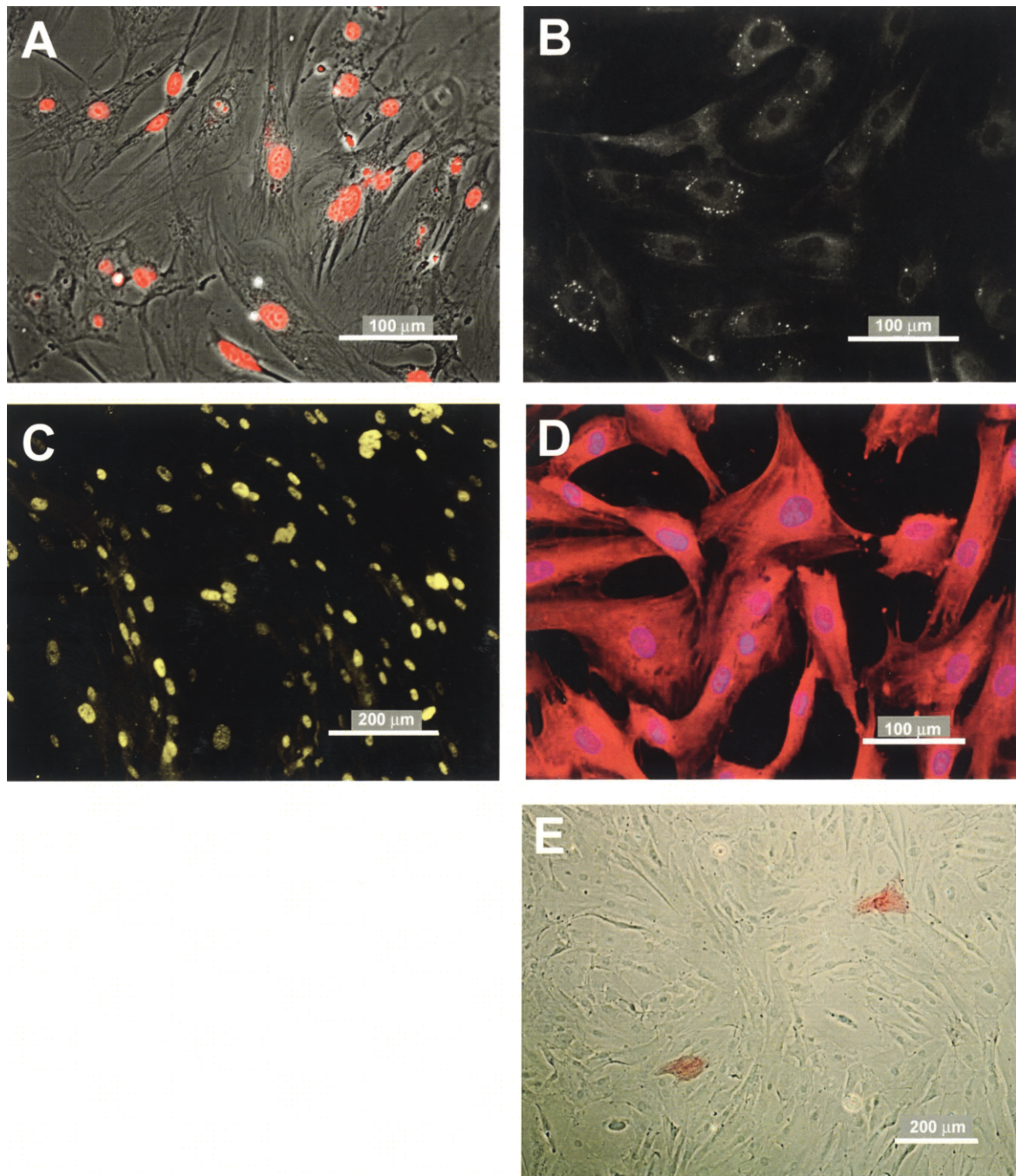


Figure 3. Immunochemical staining reveals cell proliferation, expression of characteristic Sertoli cell markers, and few myoid cells. Fluorescent microscopy of MM-HSE-3608 (passage 6) cells after treatment with 2 μ M EdU for 3 days (A) demonstrates nuclear uptake of EdU in almost all cells. Fluorescence microscopy of MM-HSE-2305 cells (passage 4) stained with AdipoRed reveals bright spots shown in grayscale that are indicative of lipid droplets (B). Immunostaining of HSE-MM-2305 cells (passage 3) for GATA-4 (C) demonstrates the expected nuclear expression pattern, whereas bisbenzamide (Hoescht) dye (blue) staining of nuclei and immunostaining for FSHr (D) is consistent with its expected cytoplasmic localization. Low detection of Vector Red from alkaline phosphatase activity (E) demonstrates that there are few myoid cells in the culture. Two red-stained myoid cells can be observed. Scale bars: 100 or 200 μ m as indicated.

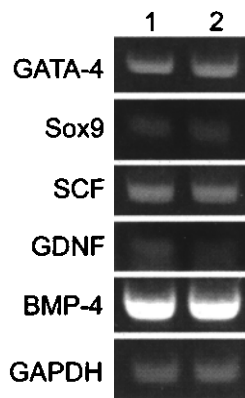


Figure 4. RT-PCR confirms cellular expression of genes that are characteristic of Sertoli cells. Lane 1 is MM-HSE-3608 cells; 2 is MM-HSE-1208.

Immunohistochemistry of Galectin-1 in Human Testis

Microphotographs of cryosections of normal adult testis stained with hematoxylin and eosin (Fig. 6A) show the structural architecture of the tubule. Sertoli and spermatogonial stem cells are surrounded by peritubular myoid cells, various stages of the differentiating germ cells fill the lumen, and Leydig cells are located in the interstitial spaces between tubules. High levels of galectin-1 staining (green) can be observed in cryosections immunostained with galectin-1 antibody (Fig. 6B) associated with the peritubular cells on the edge of the tubules, and within the tubules associated with both differentiating germ cells and Sertoli cells. Galectin-1 expression is of particular interest due to its immunosuppressive activity (28,52,55,73,74).

MM-HSE-3608 Human Sertoli Cells Display Polarity as Observed in Testes

To establish an *in vitro* human Sertoli BTB model, cells were seeded on semipermeable 24-well transwell inserts coated with fibronectin. Precoated collagen I, laminin, and fibronectin transwell inserts, uncoated inserts, and inserts coated with thick (150 μ l) or thin (30 μ l) layers of Matrigel also were tested. The effect of changing parameters such as different pore sizes (0.4, 1.0, 3.0, and 8.0 μ M), cell seeding densities, and growth media with and without FBS were examined. To compare the formation of tight junctions under the various conditions, the transwell inserts were assessed visually by observation of unequal levels of media in the apical and basolateral chambers of the transwells, by detection of the polarized secretion of protein, and by measurement of TER that is correlated positively with a more impenetrable barrier. The major problem encountered was that the Sertoli cells tended to separate from the edges of the insert and curl up. The use of either thick

or thin layers of Matrigel resulted in contraction and spheroid formation. The cells growing on fibronectin-coated transwell inserts were the only ones that were not visibly contracted from the edge of the insert, and also produced the highest TER values. As illustrated in Table 4 with MM-HSE-3608 cells (passage 4), growing the Sertoli cells on transwell inserts that were coated with fibronectin resulted in noncontracted layers forming tight junctions that reached an average of 137.1 ohms/cm² at 7 days postplating. The data are representative of three independent experiments. These TER values are similar to those reported when tight junctions were formed by rodent Sertoli cells in transwell systems in the absence of FSH and testosterone supplementation of the medium (9,29).

The formation of tight junctions was also assessed by analyses of polarized secretion of protein. Conditioned media from apical and basolateral chambers of transwell inserts seeded with Sertoli cells were collected after 3 and 7 days and the expression of galectin-1 was analyzed by SDS-PAGE followed by immunoblot. The results revealed (Fig. 7) that the galectin-1 concentration was higher in the medium from the apical compared to the basolateral chambers at both 3 and 7 days, and demonstrated the integrity of the barrier formed by the tight junctions of the confluent cells in the inserts.

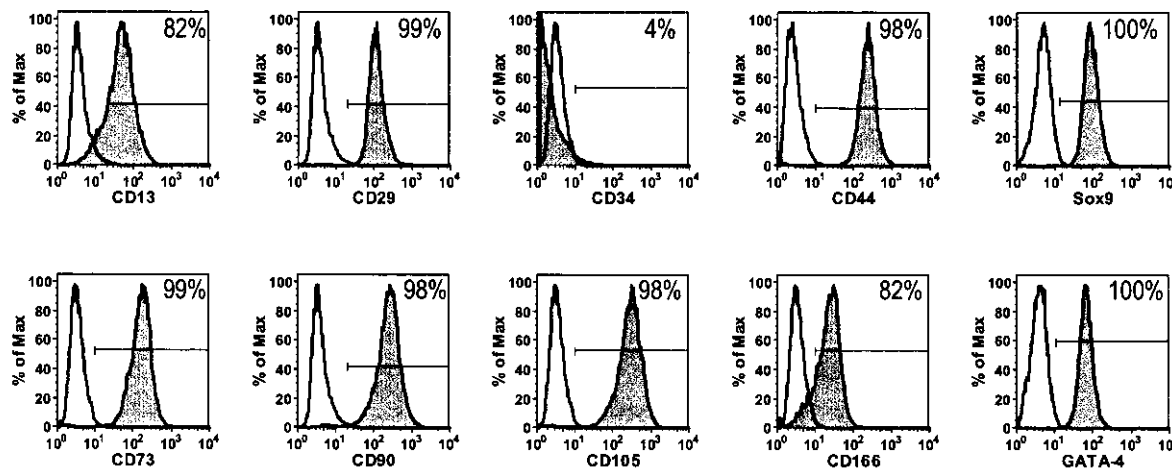
Conditioned Medium From Human Sertoli Cells Inhibits Lymphocyte Proliferation

To ascertain whether human Sertoli cells secrete immunosuppressive factors, conditioned medium was prepared from MM-HSE-2305 cells (passage 4), and the effect on human T lymphocytes (Jurkat E6-1 cells) was evaluated in a proliferation assay. There was a significant ($p < 0.001$) dose-responsive decrease in the proliferation of human T lymphocytes incubated with various concentrations of human Sertoli cell conditioned media compared to cells exposed to the same concentrations of medium conditioned by HS27 human foreskin fibroblast cell conditioned medium (Fig. 8). More than 50% of the proliferation was inhibited with the highest concentration of Sertoli cell conditioned medium.

DISCUSSION

We provide the first evidence that a small population of proliferative human Sertoli cells isolated from adult human testes can be expanded *in vitro* while retaining expression of characteristic markers and exhibiting prototypical functionality. *In vivo* Sertoli cells create the BTB that consists of specialized junctions, including tight junctions, basal ectoplasmic specializations, and desmosome-like junctions. This report also is the first to describe establishment of a tight junction barrier, a

A MM-HSE-3608



B MM-HSE-2305

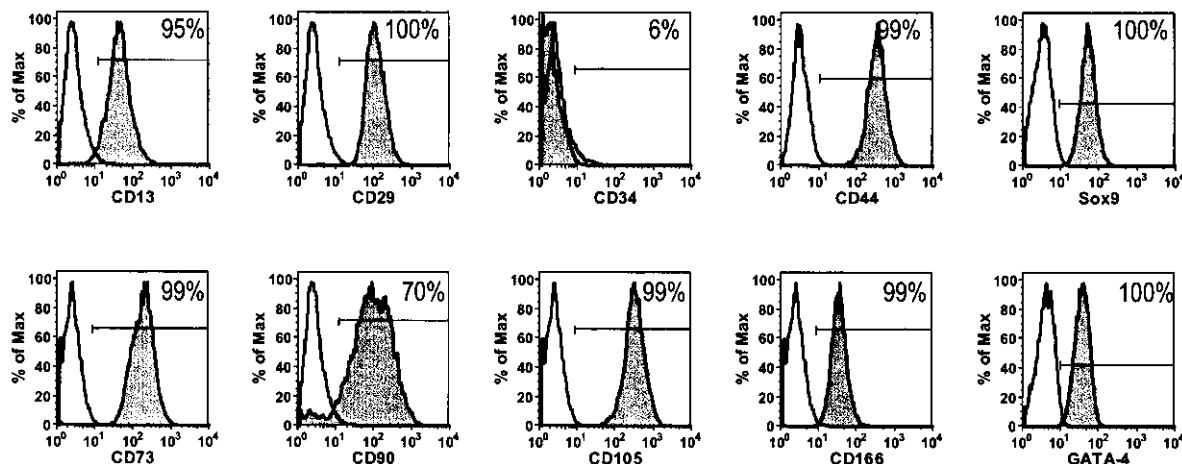


Figure 5. Flow cytometry shows more than 90% of cells at passage 3–4 express the Sertoli cell markers GATA-4 and Sox9, and less than 7% express CD34, a marker for hematopoietic and endothelial progenitor cells. Gray histograms showing antibodies staining of MM-HSE-3608 (A) and MM-HSE-2305 (B) cells for CD13, CD29, CD34, CD44, Sox9, CD73, CD90, CD105, CD166, and GATA-4 compared to that of isotype control antibodies (white histograms). The percentage of cells positively stained for each antigen is shown.

characteristic function of Sertoli cells, by isolated human Sertoli cells in vitro.

The primary human Sertoli cells were plated at high density onto transwell inserts coated with human fibronectin, an extracellular matrix protein secreted by testicular peritubular myoid cells but not by Sertoli cells (66,78). The human fibronectin facilitated the formation of stable, polarized cell monolayers that over time developed a tight junction–permeability barrier as shown by an increase in TER and by the polarized secretion of galectin-1. These data suggest that the polarized Sertoli cells were oriented so that the apical compartment of the transwells corresponded to the adluminal side of the Sertoli cell barrier because in the seminiferous tubule

the Sertoli cell tight junctions are formed adjacent to the basement membrane near the underlying myoid cells (41,65). In future studies, we plan to image proteins comprising the tight junctions in the polarized human Sertoli cells (84,85), and test the effect of FSH and testosterone supplementation on the barrier function. This system, when fully characterized, might prove to be a valuable tool as a BTB model for testing the toxicity and penetration of chemicals and drugs, and as an aid in achieving human in vitro spermatogenesis.

We analyzed expression of cell surface markers because identification of such markers specific for Sertoli cells could facilitate their purification. The Sertoli cell markers GATA-4 and Sox9 are nuclear and therefore

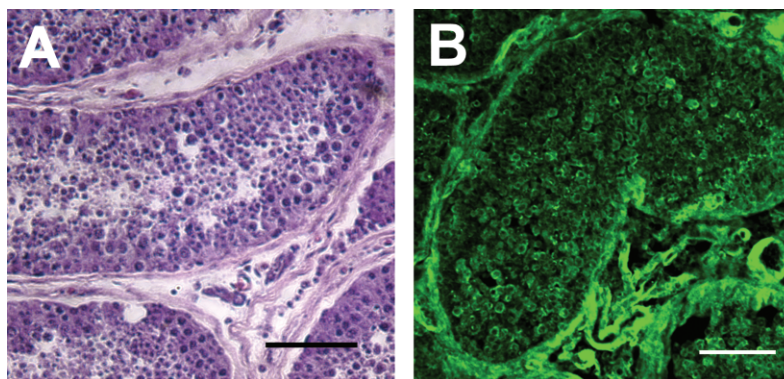


Figure 6. Immunocytochemistry of human testes sections reveals expression of galectin-1. Photomicrographs of cryosections of normal adult testis stained with hematoxylin and eosin (A), and immunostained with galectin-1 antibody (B). The hematoxylin and eosin-stained cross section of the seminiferous tubule (A) shows the structural architecture of the tubule in which Sertoli and spermatogonial stem cells are surrounded by peritubular myoid cells, and germ cells fill the lumen. Leydig cells are located in the interstitial spaces between the tubules. High levels of galectin-1 (B) staining (green) can be observed on the perimeter of the tubule, and within the tubules associated with both Sertoli cells and differentiating germ cells. Scale bars: 50 μ m.

not useful in purification of living cells. The Sertoli cells expressed several cell surface antigens that are involved in proliferation and motility, including CD166 (activated leukocyte cell adhesion molecule or ALCAM), which is primarily found on subsets of cells undergoing robust growth or migration (47,70), CD105 (endoglin), an accessory component of the receptor complex of transforming growth factor- β (TGF- β), indicative of proliferation in endothelial cells (19), and CD13, or aminopeptidase N (43). Other cell surface antigens detected such as CD29 (integrin β -1), CD44 (hyaluronan/fibronectin or MIP-1 β receptor), and CD90 (Thy-1) are adhesion molecules involved in cell-extracellular matrix or cell-cell interactions. Interestingly, CD13, CD29, CD44, CD73, CD90, CD105, and CD166 are thought to be characteristic markers for multipotent mesenchymal cells (14,40). GATA4 (32) and Sox9 (6,7) are expressed by some populations of mesenchymal stem cells. CD90 has been localized to human spermatogonia (24), and has been employed in isolation of spermatogonial stem cells (10). However, as shown our data indicate, CD90 is also expressed by human Sertoli cells, and therefore

Table 4. TER of Transwell Inserts

Well	TER/cm ²	SD
1	136.4	15.5
2	138.5	4.62
3	136.4	27.2
Mean	137.1	15.8

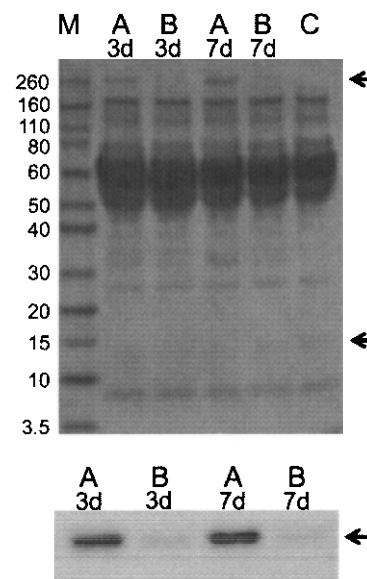


Figure 7. A Ponceau S-stained blot (upper) of conditioned media from the apical (A lanes) and bottom (B lanes) transwell chambers containing a monolayer of Sertoli cells on cell culture inserts at 3 and 7 days postplating with MW markers (M lane) on the left side is presented. Greater apical (top chamber) secretion was detected of an unidentified protein running near the 260-kDa marker on the Ponceau S-stained loading control blot (top arrow). Growth medium only as a negative control is shown in lane C. In the immunoblot (lower) greater secretion of galectin-1 into conditioned media from apical (A lanes) compared to bottom chamber (B lanes) from transwells at 3 and 7 days postplating is revealed by the bands that are at approximately 14.5 kDa (bottom arrow).

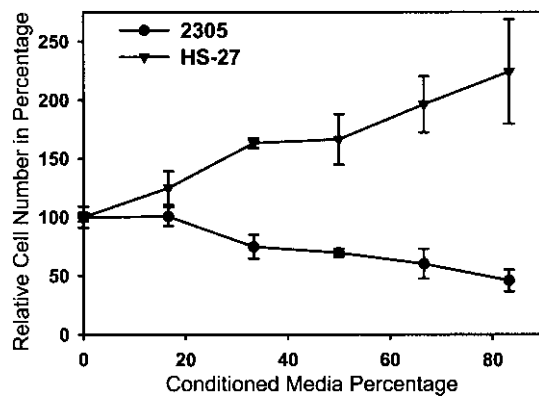


Figure 8. Conditioned media from human Sertoli cells suppress lymphocyte proliferation. Proliferation of lymphocytes was significantly decreased by conditioned media from MM-HSE-2305 Sertoli cells (two-way ANOVA, $p < 0.001$) compared to HS-27 conditioned medium. Values represent the mean \pm SD and are from three separate experiments with each concentration tested in triplicate.

would not be selective for a pure population of spermatogonial stem cells.

Expression of alkaline phosphatase, which is indicative of peritubular myoid cells, was observed at very low levels, with decreased staining with increasing number of cell passages. Possibly, the culture could be selectively enriched for the Sertoli cells because the alkaline-phosphatase-positive peritubular myoid cells are more adhesive to cell culture ware or divide more slowly than Sertoli cells.

The results provide evidence in support of active immunosuppression in the human testis. Indeed, *in vitro* cultured human Sertoli cells retained immunosuppressive capability, as their conditioned media inhibited the proliferation of T lymphocytes. The inhibitory effect of the primary human Sertoli cell conditioned media on the proliferation of human Jurkat E.6 T lymphocytes was similar in magnitude to that we observed with rat T lymphocytes and rat Sertoli cell conditioned media (76). The data also are in accordance with previous reports of the inhibition of proliferation of lymphocytes by rodent Sertoli cell conditioned media (12,60). Evidence of active immunosuppression by our primary human Sertoli cells may be especially important for potential therapeutic applications because data from animal studies indicate that Sertoli cell lines lack immunosuppressive properties (15).

Our description of the polarized expression of galectin-1 by the human Sertoli cells corroborates the previous observation of the regulated expression of galectin-1 during the spermatogenic cycle of rats (13). We also observed localization of galectin-1 *in vivo* in the adluminal compartment of the human seminiferous tubule, con-

firmed the previously reported cytoplasmic and nuclear expression of galectin-1 by human Sertoli cells (83). The perimeter of the seminiferous tubule where the peritubular cells are located appeared to have the greatest concentration of galectin-1. Fibronectin, which is secreted by the peritubular myoid cells (78), has been found to be a ligand of galectin-1 (50).

The immunosuppressive properties of galectin-1, including the ability of this glycan-binding protein to regulate dendritic cell physiology and T cell fate, have been well established (55). Thus, the data suggest that galectin-1 could potentially have an active role in conferring an immune-privileged status to the human testis.

Although it has long been thought that mammalian Sertoli cells do not divide postpuberty (48,49,62), recently this view has been challenged (1,75). Our results show that human adult Sertoli cells retain the ability to divide postpuberty and possess immunoregulatory activity.

Proliferation of adult murine Sertoli cells *in vitro* in the absence of specific hormonal supplementation was found to be associated with a 70% decrease in expression of the cell cycle inhibitor CDKN1B (P27kip1) and a twofold increase in the levels of the proliferation inducer ID2 (1). Whether adult Sertoli cells resumed proliferation *in vitro* in the absence of specific hormone supplementation or if we isolated a subpopulation of Sertoli cell progenitor cells is not clear. In rats FSH has been shown to affect Sertoli and germ cell proliferation in an age-dependent manner (42). Our data appear consistent with results from a study of Sertoli cell differentiation in adult Djungarian hamsters that included analyses of cell proliferation, localization of junctional proteins, and expression of maturation markers and found the adult Sertoli cells were not terminally differentiated but existed in a transitional state, exhibiting both undifferentiated and differentiated features (72). Our results suggest that the proliferative adult human Sertoli cells may share some characteristics with mesenchymal stem cells.

Recently, a putative population of mesenchymal stem cells was isolated from adult human testes that when cultured using specific differentiation medium differentiated into adipogenic, osteogenic, and chondrogenic cells (21) exhibiting broad plasticity. The testicular mesenchymal cells expressed CD105, CD166, CD73, and CD90, and had morphology similar to that of the functional primary human Sertoli cells.

Culture conditions including confluency, transmembrane potential, growth hormones, extracellular matrix, and other characteristics of the microenvironment affect cell differentiation (3,54,69,80). Our results demonstrate that after isolation and culture under the conditions described, the proliferative primary human testicular cells exhibit characteristics specific to human Sertoli cells,

which are the only testicular cells that form tight junctions, express Sox9, or the receptor for FSH.

In summary, our results demonstrated the retention of phenotypic characteristics and functionality of primary human Sertoli cells isolated from adult testes after their *in vitro* expansion and cryopreservation and, therefore, provide evidence of potential utility in spermatogenesis and infertility research (86), and reproductive toxicology (44,53). Greater availability of primary human Sertoli cells may facilitate studies of Sertoli cell maturation that is thought to be a factor in some disorders of testicular function (62). Because of their robust proliferative ability and unique biological role (15) these primary human Sertoli cells also could have applications in cell therapy such as in treatment of infertility (63), or potentially in nurturing and protecting coimplanted stem cells (23,82).

ACKNOWLEDGMENTS: *This work was supported by funding from the National Institutes of Health (National Institute of Child Health and Human Development 2R44HD042333 to A.T., 1R43HD056620 to C.M.J., and 5R01HD056034 to C.Y.C.) and the UCLA Neurotrauma Research Program (505624-19900 awarded to A.T.). We acknowledge use of tissues procured by the National Disease Research Interchange (NDRI) with support from NIH (2 U42 RR006042-13). The assistance of Kimberly Topp of the UCSF Physical Therapy & Rehabilitation Science Department with the electron microscopy, Richelle A. Hemendinger of the Carolinas Medical Center, in Charlotte, NC with Sox9 immunoblots, JoDee Fisher and Caroline Miller of the Histology Core Laboratory of the J. David Gladstone Institutes with the histology, and Kurt Thorn, the Director of the UCSF Nikon Imaging Center with the fluorescence microscopy is gratefully acknowledged. At the time of the study, Kitty Chui, Alpa Trivedi, Ai Lam Thuy Huynh, and Constance M. John were employees of MandalMed, Inc., and C. Yan Cheng was an Advisor. All of the former own stock in MandalMed. Paul F. Dazin was a consultant to MandalMed, and James B. Mitchell was an employee of Lonza, Walkersville.*

REFERENCES

- Ahmed, E. A.; Barten-van Rijbroek, A. D.; Kal, H. B.; Sadri-Ardekani, H.; Mizrak, S. C.; van Pelt, A. M.; de Rooij, D. G. Proliferative activity *in vitro* and DNA repair indicate that adult mouse and human Sertoli cells are not terminally differentiated, quiescent cells. *Biol. Reprod.* 80:1084–1091; 2009.
- Anthony, C.; Skinner, M. K. Cytochemical and biochemical characterization of testicular peritubular myoid cells. *Biol. Reprod.* 40:811–823; 1989.
- Benton, G.; George, J.; Kleinman, H. K.; Arnautova, I. P. Advancing science and technology via 3D culture on basement membrane matrix. *J. Cell. Physiol.* 221:18–25; 2009.
- Bockers, T. M.; Nieschlag, E.; Kreutz, M. R.; Bergmann, M. Localization of follicle-stimulating hormone (FSH) immunoreactivity and hormone receptor mRNA in testicular tissue of infertile men. *Cell Tissue Res.* 278:595–600; 1994.
- Bustin, S. A. Absolute quantification of mRNA using real-time reverse transcription polymerase chain reaction assays. *J. Mol. Endocrinol.* 25:169–193; 2000.
- Campbell, J. J.; Lee, D. A.; Bader, D. L. Dynamic compressive strain influences chondrogenic gene expression in human mesenchymal stem cells. *Biorheology* 43:455–470; 2006.
- Chang, Y.; Ueng, S. W.; Lin-Chao, S.; Chao, C. C. Involvement of Gas7 along the ERK1/2 MAP kinase and SOX9 pathway in chondrogenesis of human marrow-derived mesenchymal stem cells. *Osteoarthritis Cartilage* 16:1403–1412; 2008.
- Cheng, C. Y.; Mruk, D. D. An intracellular trafficking pathway in the seminiferous epithelium regulating spermatogenesis: A biochemical and molecular perspective. *Crit. Rev. Biochem. Mol. Biol.* 44:245–263; 2009.
- Chung, N. P.; Cheng, C. Y. Is cadmium chloride-induced inter-Sertoli tight junction permeability barrier disruption a suitable *in vitro* model to study the events of junction disassembly during spermatogenesis in the rat testis? *Endocrinology* 142:1878–1888; 2001.
- Conrad, S.; Renninger, M.; Hennenlotter, J.; Wiesner, T.; Just, L.; Bonin, M.; Aicher, W.; Buhning, H. J.; Mattheus, U.; Mack, A.; Wagner, H. J.; Minger, S.; Matzkies, M.; Reppel, M.; Hescheler, J.; Sievert, K. D.; Stenzl, A.; Skutella, T. Generation of pluripotent stem cells from adult human testis. *Nature* 456:344–349; 2008.
- Davidoff, M. S.; Middendorff, R.; Koeva, Y.; Pusch, W.; Jezek, D.; Muller, D. Glial cell line-derived neurotrophic factor (GDNF) and its receptors GFR α -1 and GFR α -2 in the human testis. *Ital. J. Anat. Embryol.* 106(2 Suppl. 2):173–180; 2001.
- De Cesaris, P.; Filippini, A.; Cervelli, C.; Riccioli, A.; Muci, S.; Starace, G.; Stefanini, M.; Ziparo, E. Immunosuppressive molecules produced by Sertoli cells cultured *in vitro*: Biological effects on lymphocytes. *Biochem. Biophys. Res. Commun.* 186:1639–1646; 1992.
- Dettin, L.; Rubinstein, N.; Aoki, A.; Rabinovich, G. A.; Maldonado, C. A. Regulated expression and ultrastructural localization of galectin-1, a proapoptotic beta-galactoside-binding lectin, during spermatogenesis in rat testis. *Biol. Reprod.* 68:51–59; 2003.
- Dominici, M.; Le Blanc, K.; Mueller, I.; Slaper-Cortenbach, I.; Marini, F.; Krause, D.; Deans, R.; Keating, A.; Prockop, D.; Horwitz, E. Minimal criteria for defining multipotent mesenchymal stromal cells. The International Society for Cellular Therapy position statement. *Cytotherapy* 8:315–317; 2006.
- Dufour, J. M.; Dass, B.; Halley, K. R.; Korbitt, G. S.; Dixon, D. E.; Rajotte, R. V. Sertoli cell line lacks the immunoprotective properties associated with primary Sertoli cells. *Cell Transplant.* 17:525–534; 2008.
- Dufour, J. M.; Rajotte, R. V.; Korbitt, G. S.; Emerich, D. F. Harnessing the immunomodulatory properties of Sertoli cells to enable xenotransplantation in type I diabetes. *Immunol. Invest.* 32:275–297; 2003.
- Fallarino, F.; Luca, G.; Calvitti, M.; Mancuso, F.; Nastruzzi, C.; Fioretti, M. C.; Grohmann, U.; Becchetti, E.; Burgevin, A.; Kratzer, R.; van Endert, P.; Boon, L.; Puccetti, P.; Calafiore, R. Therapy of experimental type I diabetes by isolated Sertoli cell xenografts alone. *J. Exp. Med.* 206:2511–2526; 2009.
- Filippini, A.; Riccioli, A.; Padula, F.; Lauretti, P.; D'Alessio, A.; De Cesaris, P.; Gandini, L.; Lenzi, A.; Ziparo, E. Control and impairment of immune privilege in the testis and in semen. *Hum. Reprod. Update* 7:444–449; 2001.

19. Fonsatti, E.; Maio, M. Highlights on endoglin (CD105): From basic findings towards clinical applications in human cancer. *J. Transl. Med.* 2:18; 2004.
20. Frojzman, K.; Harley, V. R.; Pelliniemi, L. J. Sox9 protein in rat Sertoli cells is age and stage dependent. *Histochem. Cell Biol.* 113:31–36; 2000.
21. Gonzalez, R.; Griparic, L.; Vargas, V.; Burgee, K.; Santacruz, P.; Anderson, R.; Schiewe, M.; Silva, F.; Patel, A. A putative mesenchymal stem cells population isolated from adult human testes. *Biochem. Biophys. Res. Commun.* 385:570–575; 2009.
22. Griswold, M. D. The central role of Sertoli cells in spermatogenesis. *Semin. Cell Dev. Biol.* 9:411–416; 1998.
23. Halberstadt, C.; Emerich, D.; Gores, P. Use of Sertoli cell transplants to provide local immunoprotection for tissue grafts. *Expert Opin. Biol. Ther.* 4:813–825; 2004.
24. He, Z.; Kokkinaki, M.; Jiang, J.; Dobrinski, I.; Dym, M. Isolation, Characterization, and culture of human spermatogonia. *Biol. Reprod.* 82:363–372; 2009.
25. Hemendinger, R. A.; Gores, P.; Blacksten, L.; Harley, V.; Halberstadt, C. Identification of a specific Sertoli cell marker, Sox9, for use in transplantation. *Cell Transplant.* 11:499–505; 2002.
26. Hofmann, M. C. Gdnf signaling pathways within the mammalian spermatogonial stem cell niche. *Mol. Cell. Endocrinol.* 288:95–103; 2008.
27. Hu, J.; Chen, Y. X.; Wang, D.; Qi, X.; Li, T. G.; Hao, J.; Mishina, Y.; Garbers, D. L.; Zhao, G. Q. Developmental expression and function of Bmp4 in spermatogenesis and in maintaining epididymal integrity. *Dev. Biol.* 276:158–171; 2004.
28. Ilarregui, J. M.; Croci, D. O.; Bianco, G. A.; Toscano, M. A.; Salatino, M.; Vermeulen, M. E.; Geffner, J. R.; Rabinovich, G. A. Tolerogenic signals delivered by dendritic cells to T cells through a galectin-1-driven immunoregulatory circuit involving interleukin 27 and interleukin 10. *Nat. Immunol.* 10:981–991; 2009.
29. Janecki, A.; Jakubowiak, A.; Steinberger, A. Regulation of transepithelial electrical resistance in two-compartment Sertoli cell cultures: In vitro model of the blood-testis barrier. *Endocrinology* 129:1489–1496; 1991.
30. Kent, J.; Wheatley, S. C.; Andrews, J. E.; Sinclair, A. H.; Koopman, P. A male-specific role for SOX9 in vertebrate sex determination. *Development* 122:2813–2822; 1996.
31. Kerr, J. B.; Mayberry, R. A.; Irby, D. C. Morphometric studies on lipid inclusions in Sertoli cells during the spermatogenic cycle in the rat. *Cell Tissue Res.* 236:699–709; 1984.
32. Khan, M.; Akhtar, S.; Mohsin, S.; Khan, S. N.; Riazuddin, S. Growth factor preconditioning increases the function of diabetes-impaired mesenchymal stem cells. *Stem Cells Dev.* 20(1):67–75; 2011.
33. Kobayashi, A.; Chang, H.; Chaboissier, M. C.; Schedl, A.; Behringer, R. R. Sox9 in testis determination. *Ann. NY Acad. Sci.* 1061:9–17; 2005.
34. Kojima, Y.; Hayashi, Y.; Mizuno, K.; Sasaki, S.; Fukui, Y.; Koopman, P.; Morohashi, K.; Kohri, K. Up-regulation of SOX9 in human sex-determining region on the Y chromosome (SRY)-negative XX males. *Clin. Endocrinol.* 68:791–799; 2008.
35. Koopman, P. Sry and Sox9: Mammalian testis-determining genes. *Cell. Mol. Life Sci.* 55:839–856; 1999.
36. Koopman, P. Sry, Sox9 and mammalian sex determination. *EXS* (91):25–56; 2001.
37. Korbitt, G. S.; Suarez-Pinzon, W. L.; Power, R. F.; Rajotte, R. V.; Rabinovitch, A. Testicular Sertoli cells exert both protective and destructive effects on syngeneic islet grafts in non-obese diabetic mice. *Diabetologia* 43:474–480; 2000.
38. LaVoie, H. A. The role of GATA in mammalian reproduction. *Exp. Biol. Med.* (Maywood) 228:1282–1290; 2003.
39. Lipshultz, L. I.; Murthy, L.; Tindall, D. J. Characterization of human Sertoli cells in vitro. *J. Clin. Endocrinol. Metab.* 55:228–237; 1982.
40. Liu, F.; Akiyama, Y.; Tai, S.; Maruyama, K.; Kawaguchi, Y.; Muramatsu, K.; Yamaguchi, K. Changes in the expression of CD106, osteogenic genes, and transcription factors involved in the osteogenic differentiation of human bone marrow mesenchymal stem cells. *J. Bone Miner. Metab.* 26:312–320; 2008.
41. Lui, W. Y.; Mruk, D.; Lee, W. M.; Cheng, C. Y. Sertoli cell tight junction dynamics: Their regulation during spermatogenesis. *Biol. Reprod.* 68:1087–1097; 2003.
42. Meachem, S. J.; Ruwanpura, S. M.; Ziolkowski, J.; Ague, J. M.; Skinner, M. K.; Loveland, K. L. Developmentally distinct in vivo effects of FSH on proliferation and apoptosis during testis maturation. *J. Endocrinol.* 186:429–446; 2005.
43. Mina-Osorio, P. The moonlighting enzyme CD13: Old and new functions to target. *Trends Mol. Med.* 14:361–371; 2008.
44. Moffit, J. S.; Bryant, B. H.; Hall, S. J.; Boekelheide, K. Dose-dependent effects of Sertoli cell toxicants 2,5-hexanedione, carbendazim, and mono-(2-ethylhexyl) phthalate in adult rat testis. *Toxicol. Pathol.* 35:719–727; 2007.
45. Morais da Silva, S.; Hacker, A.; Harley, V.; Goodfellow, P.; Swain, A.; Lovell-Badge, R. Sox9 expression during gonadal development implies a conserved role for the gene in testis differentiation in mammals and birds. *Nat. Genet.* 14:62–68; 1996.
46. Ng, L. J.; Wheatley, S.; Muscat, G. E.; Conway-Campbell, J.; Bowles, J.; Wright, E.; Bell, D. M.; Tam, P. P.; Cheah, K. S.; Koopman, P. SOX9 binds DNA, activates transcription, and coexpresses with type II collagen during chondrogenesis in the mouse. *Dev. Biol.* 183:108–121; 1997.
47. Ofori-Acquah, S. F.; King, J. A. Activated leukocyte cell adhesion molecule: A new paradox in cancer. *Transl. Res.* 151:122–128; 2008.
48. Orth, J. M. Proliferation of Sertoli cells in fetal and post-natal rats: A quantitative autoradiographic study. *Anat. Rec.* 203:485–492; 1982.
49. Orth, J. M.; Gunsalus, G. L.; Lamperti, A. A. Evidence from Sertoli cell-depleted rats indicates that spermatid number in adults depends on numbers of Sertoli cells produced during perinatal development. *Endocrinology* 122:787–794; 1988.
50. Ozeki, Y.; Matsui, T.; Yamamoto, Y.; Funahashi, M.; Hamako, J.; Titani, K. Tissue fibronectin is an endogenous ligand for galectin-1. *Glycobiology* 5:255–261; 1995.
51. Paniagua, R.; Rodriguez, M. C.; Nistal, M.; Fraile, B.; Amat, P. Changes in the lipid inclusion/Sertoli cell cytoplasm area ratio during the cycle of the human seminiferous epithelium. *J. Reprod. Fertil.* 80:335–341; 1987.
52. Perillo, N. L.; Pace, K. E.; Seilhamer, J. J.; Baum, L. G. Apoptosis of T cells mediated by galectin-1. *Nature* 378:736–738; 1995.
53. Petersen, C.; Soder, O. The Sertoli cell—a hormonal target and ‘super’ nurse for germ cells that determines testicular size. *Horm. Res.* 66:153–161; 2006.

54. Pretzer, D.; Ghaida, J. A.; Rune, G. M. Growth factors (EGF, IGF-I) modulate the morphological differentiation of adult marmoset (*Callithrix jacchus*) Sertoli cells in vitro. *J. Androl.* 15:398–409; 1994.
55. Rabinovich, G. A.; Toscano, M. A. Turning 'sweet' on immunity: Galectin–glycan interactions in immune tolerance and inflammation. *Nat. Rev. Immunol.* 9:338–352; 2009.
56. Sanberg, P. R.; Borlongan, C. V.; Saporta, S.; Cameron, D. F. Testis-derived Sertoli cells survive and provide localized immunoprotection for xenografts in rat brain. *Nat. Biotechnol.* 14:1692–1695; 1996.
57. Sandlow, J. I.; Feng, H. L.; Cohen, M. B.; Sandra, A. Expression of c-KIT and its ligand, stem cell factor, in normal and subfertile human testicular tissue. *J. Androl.* 17:403–408; 1996.
58. Santemma, V.; Rosati, P.; Guerzoni, C.; Mariani, S.; Beligotti, F.; Magnanti, M.; Garufi, G.; Galoni, T.; Fabbrini, A. Human Sertoli cells in vitro: Morphological features and androgen-binding protein secretion. *J. Steroid Biochem. Mol. Biol.* 43:423–429; 1992.
59. Selawry, H.; Whittington, K. Extended allograft survival of islets grafted in the intra-abdominally placed testis. *Diabetes* 33:405–406; 1984.
60. Selawry, H. P.; Kotb, M.; Herrod, H. G.; Lu, Z. N. Production of a factor, or factors, suppressing IL-2 production and T cell proliferation by Sertoli cell-enriched preparations. A potential role for islet transplantation in an immunologically privileged site. *Transplantation* 52:846–850; 1991.
61. Shamekh, R.; El-Badri, N. S.; Saporta, S.; Pascual, C.; Sanberg, P. R.; Cameron, D. F. Sertoli cells induce systemic donor-specific tolerance in xenogenic transplantation model. *Cell Transplant.* 15:45–53; 2006.
62. Sharpe, R. M.; McKinnell, C.; Kivlin, C.; Fisher, J. S. Proliferation and functional maturation of Sertoli cells, and their relevance to disorders of testis function in adulthood. *Reproduction* 125:769–784; 2003.
63. Shinohara, T.; Orwig, K. E.; Avarbock, M. R.; Brinster, R. L. Restoration of spermatogenesis in infertile mice by Sertoli cell transplantation. *Biol. Reprod.* 68:1064–1071; 2003.
64. Siu, M. K.; Cheng, C. Y. Dynamic cross-talk between cells and the extracellular matrix in the testis. *Bioessays* 26:978–992; 2004.
65. Siu, M. K.; Cheng, C. Y. Extracellular matrix and its role in spermatogenesis. *Adv. Exp. Med. Biol.* 636:74–91; 2008.
66. Skinner, M. K.; Stallard, B.; Anthony, C. T.; Griswold, M. D. Cellular localization of fibronectin gene expression in the seminiferous tubule. *Mol. Cell. Endocrinol.* 66:45–52; 1989.
67. Strohmeier, T.; Reese, D.; Press, M.; Ackermann, R.; Hartmann, M.; Slamon, D. Expression of the c-kit proto-oncogene and its ligand stem cell factor (SCF) in normal and malignant human testicular tissue. *J. Urol.* 153:511–515; 1995.
68. Suarez-Pinzon, W.; Korbitt, G. S.; Power, R.; Hooton, J.; Rajotte, R. V.; Rabinovitch, A. Testicular Sertoli cells protect islet beta-cells from autoimmune destruction in NOD mice by a transforming growth factor-beta1-dependent mechanism. *Diabetes* 49:1810–1818; 2000.
69. Sundelacruz, S.; Levin, M.; Kaplan, D. L. Role of membrane potential in the regulation of cell proliferation and differentiation. *Stem Cell Rev.* 5:231–246; 2009.
70. Swart, G. W. Activated leukocyte cell adhesion molecule (CD166/ALCAM): Developmental and mechanistic aspects of cell clustering and cell migration. *Eur. J. Cell Biol.* 81(6):313–321; 2002.
71. Tarnok, A.; Ulrich, H.; Bocsi, J. Phenotypes of stem cells from diverse origin. *Cytometry A* 77:6–10; 2010.
72. Tarulli, G. A.; Stanton, P. G.; Lerchl, A.; Meachem, S. J. Adult Sertoli cells are not terminally differentiated in the Djungarian hamster: Effect of FSH on proliferation and junction protein organization. *Biol. Reprod.* 74:798–806; 2006.
73. Toscano, M. A.; Bianco, G. A.; Ilarregui, J. M.; Croci, D. O.; Correale, J.; Hernandez, J. D.; Zwirner, N. W.; Poirier, F.; Riley, E. M.; Baum, L. G.; Rabinovich, G. A. Differential glycosylation of TH1, TH2 and TH-17 effector cells selectively regulates susceptibility to cell death. *Nat. Immunol.* 8:825–834; 2007.
74. Toscano, M. A.; Commodaro, A. G.; Ilarregui, J. M.; Bianco, G. A.; Liberman, A.; Serra, H. M.; Hirabayashi, J.; Rizzo, L. V.; Rabinovich, G. A. Galectin-1 suppresses autoimmune retinal disease by promoting concomitant Th2- and T regulatory-mediated anti-inflammatory responses. *J. Immunol.* 176:6323–6332; 2006.
75. Trivedi, A.; Huynh, A.; Hemendinger, R.; Noble-Haeusslein, L.; John, C. M. Isolation of proliferative human Sertoli cells. Society for Neuroscience Meeting, San Diego, CA; 2007.
76. Trivedi, A.; Igarashi, T.; Hall, D. E.; Love, J.; John, C. M.; Noble, L. J. Cell based delivery of NT-3 in injured rat spinal cord. Society for Neuroscience Meeting, San Diego, CA; 2001.
77. Trivedi, A. A.; Igarashi, T.; Compagnone, N.; Fan, X.; Hsu, J. Y.; Hall, D. E.; John, C. M.; Noble-Haeusslein, L. J. Suitability of allogeneic Sertoli cells for ex vivo gene delivery in the injured spinal cord. *Exp. Neurol.* 198:88–100; 2006.
78. Tung, P. S.; Skinner, M. K.; Fritz, I. B. Fibronectin synthesis is a marker for peritubular cell contaminants in Sertoli cell-enriched cultures. *Biol. Reprod.* 30:199–211; 1984.
79. Viger, R. S.; Mertineit, C.; Trasler, J. M.; Nemer, M. Transcription factor GATA-4 is expressed in a sexually dimorphic pattern during mouse gonadal development and is a potent activator of the Mullerian inhibiting substance promoter. *Development* 125:2665–2675; 1998.
80. Votteler, M.; Kluger, P. J.; Walles, H.; Schenke-Layland, K. Stem cell microenvironments—unveiling the secret of how stem cell fate is defined. *Macromol. Biosci.* 210(11):1302–1315; 2010.
81. Wang, H.; Wang, H.; Xiong, W.; Chen, Y.; Ma, Q.; Ma, J.; Ge, Y.; Han, D. Evaluation on the phagocytosis of apoptotic spermatogenic cells by Sertoli cells in vitro through detecting lipid droplet formation by Oil Red O staining. *Reproduction* 132:485–492; 2006.
82. Willing, A. E.; Othberg, A. I.; Saporta, S.; Anton, A.; Sinibaldi, S.; Poulos, S. G.; Cameron, D. F.; Freeman, T. B.; Sanberg, P. R. Sertoli cells enhance the survival of co-transplanted dopamine neurons. *Brain Res.* 822:246–250; 1999.
83. Wollina, U.; Schreiber, G.; Gornig, M.; Feldrappe, S.; Burchert, M.; Gabius, H. J. Sertoli cell expression of galectin-1 and -3 and accessible binding sites in normal human testis and Sertoli cell only-syndrome. *Histol. Histopathol.* 14:779–784; 1999.

84. Xia, W.; Mruk, D. D.; Cheng, C. Y. C-type natriuretic peptide regulates blood-testis barrier dynamics in adult rat testes. *Proc. Natl. Acad. Sci. USA* 104:3841–3846; 2007.
85. Yan, H. H.; Cheng, C. Y. Blood–testis barrier dynamics are regulated by an engagement/disengagement mechanism between tight and adherens junctions via peripheral adaptors. *Proc. Natl. Acad. Sci. USA* 102:11722–11727; 2005.
86. Yan, H. H.; Mruk, D. D.; Cheng, C. Y. Junction restructuring and spermatogenesis: the biology, regulation, and implication in male contraceptive development. *Curr. Top. Dev. Biol.* 80:57–92; 2008.
87. Yazama, F. Continual maintenance of the blood–testis barrier during spermatogenesis: The intermediate compartment theory revisited. *J. Reprod. Dev.* 54:299–305; 2008.

